doi:10.1093/brain/awp323 Brain 2010: 133; 923–940 | 923

BRAIN
A JOURNAL OF NEUROLOGY

Oculopalatal tremor explained by a model of inferior olivary hypertrophy and cerebellar plasticity

Aasef G. Shaikh,[1] Simon Hong,[2] Ke Liao,[3] Jing Tian,[1] David Solomon,[1] David S. Zee,[1] R. John Leigh[3] and Lance M. Optican[2]

1 Department of Neurology, The Johns Hopkins University, Baltimore, MD 21287, USA
2 Laboratory of Sensorimotor Research, National Eye Institute, NIH, DHHS Bethesda, MD 20892-4435, USA
3 Department of Neurology, Veterans Affairs Medical Center and Case Western Reserve University, Cleveland, OH 44106-1702, USA

Correspondence to: Lance M. Optican, PhD,
49 Convent Drive, Room 2A50,
Bethesda, MD 20892-4435,
USA
E-mail: lanceoptican@nih.gov

The inferior olivary nuclei clearly play a role in creating oculopalatal tremor, but the exact mechanism is unknown. Oculopalatal tremor develops some time after a lesion in the brain that interrupts inhibition of the inferior olive by the deep cerebellar nuclei. Over time the inferior olive gradually becomes hypertrophic and its neurons enlarge developing abnormal soma-somatic gap junctions. However, results from several experimental studies have confounded the issue because they seem inconsistent with a role for the inferior olive in oculopalatal tremor, or because they ascribe the tremor to other brain areas. Here we look at 3D binocular eye movements in 15 oculopalatal tremor patients and compare their behaviour to the output of our recent mathematical model of oculopalatal tremor. This model has two mechanisms that interact to create oculopalatal tremor: an oscillator in the inferior olive and a modulator in the cerebellum. Here we show that this dual mechanism model can reproduce the basic features of oculopalatal tremor and plausibly refute the confounding experimental results. Oscillations in all patients and simulations were aperiodic, with a complicated frequency spectrum showing dominant components from 1 to 3 Hz. The model's synchronized inferior olive output was too small to induce noticeable ocular oscillations, requiring amplification by the cerebellar cortex. Simulations show that reducing the influence of the cerebellar cortex on the oculomotor pathway reduces the amplitude of ocular tremor, makes it more periodic and pulse-like, but leaves its frequency unchanged. Reducing the coupling among cells in the inferior olive decreases the oscillation's amplitude until they stop (at ~20% of full coupling strength), but does not change their frequency. The dual-mechanism model accounts for many of the properties of oculopalatal tremor. Simulations suggest that drug therapies designed to reduce electrotonic coupling within the inferior olive or reduce the disinhibition of the cerebellar cortex on the deep cerebellar nuclei could treat oculopalatal tremor. We conclude that oculopalatal tremor oscillations originate in the hypertrophic inferior olive and are amplified by learning in the cerebellum.

Keywords: vestibular; gap junction; connexin; motor disorders; eye movement
Abbreviations: ICA = independent component analysis; OPT = oculopalatal tremor

Received July 28, 2009. Accepted November 12, 2009. Advance Access publication January 15, 2010

Introduction

Symptomatic oculopalatal tremor (OPT) is characterized by smooth, aperiodic, low frequency (1–3 Hz) oscillations of the eyes, palate and occasionally other muscles (Deuschl *et al.*, 1994*a*; Leigh and Zee, 2006). OPT develops some time (usually weeks to months) after a lesion in the Guillain–Mollaret triangle, a pathway from the deep cerebellar nuclei to the contralateral red nucleus, then to the inferior olive and back to the cerebellum (Guillain and Mollaret, 1931) (Fig. 1A). More recent evidence suggests that the red nucleus is not involved in eye movements and that it is a lesion of the central tegmental tract that leads to OPT by interrupting the pathway from the deep cerebellar nuclei through the superior cerebellar peduncle via the central tegmental tract to the inferior olive (Matsuo and Ajax, 1979; Deuschl *et al.*, 1990; Leigh and Zee, 2006). If the lesion involves the vestibulo-cerebellar output, then the vestibular nuclei correspond to the deep cerebellar nuclei. The pathway would then go from the vestibular Purkinje cells via the inferior cerebellar peduncle to the vestibular nuclei, and then to the inferior olive (Barmack, 2003).

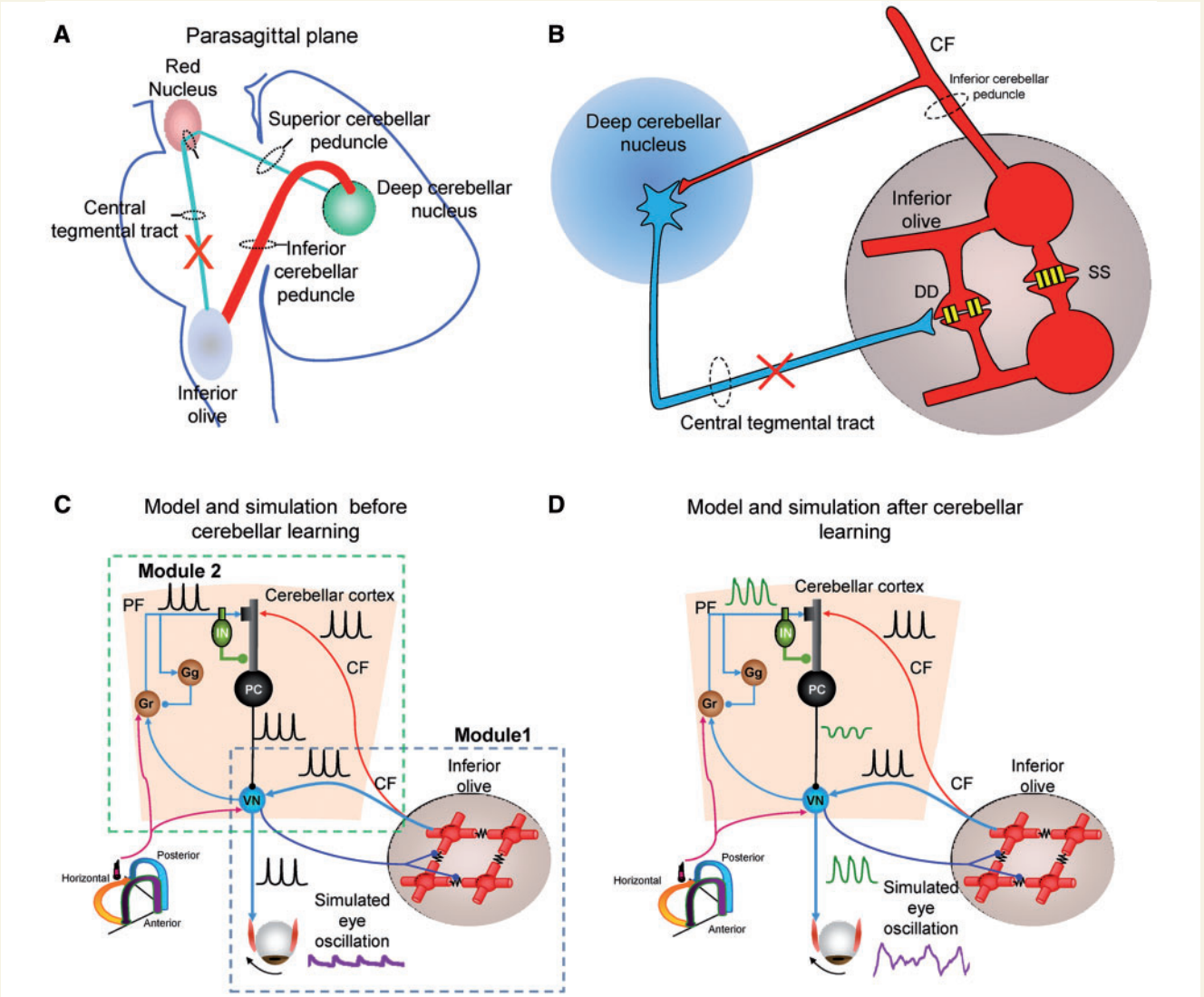

Figure 1 Schematic representation of the Guillain–Mollaret triangle formed by connections between the deep cerebellar nuclei and contralateral inferior olive, which pass near the red nucleus (**A**). The conduction strength through the dendro-dendritic gap junctions (schematized with yellow connexon channels; DD) between adjacent inferior olivary neurons are inhibited by projections from the deep cerebellar nuclei (blue projection) (**B**). Lesions in the Guillain–Mollaret triangle (red X in **A** and **B**) also result in hypertrophy of inferior olive neurons causing development of abnormal soma-somatic gap junction. Schematic representation of a model for classical delay conditioning (**C** and **D**). Model and traces from simulations after inferior olive hypertrophy but before cerebellar learning (**C**). Inferior olive and cerebellar modules after hypertrophy and learning (**D**). Lower left corner shows icon for semicircular canals (**C** and **D**). Simulated membrane potentials (black), eye oscillations (magenta). CF = climbing fibres; PF = parallel fibres; DD = dendro-dendritic gap junction; SS = soma-somatic gap junction; Gr = granule cell layer; IN = interneurons; PC = Purkinje neurons.

A key feature for our hypothesis is based on the existence of dendro-dendritic gap junctions (Sotelo *et al.*, 1974) and electrotonic coupling (Llinas *et al.*, 1974) among inferior olive neurons. The critical cause of OPT is presumed to be the removal of inhibition of the electrotonic gap junctions in the inferior olive (Fig. 1B) (Angaut and Sotelo, 1989; De Zeeuw *et al.*, 1989; Ruigrok *et al.*, 1990, 1997). Weeks to months after the lesion, the inferior olive nuclei become hypertrophic and inferior olive neurons enlarge, developing abnormal soma-somatic gap junctions (Koeppen *et al.*, 1980; Sperling and Herrmann Jr, 1985; Birbamer *et al.*, 1994; Deuschl *et al.*, 1994*a*; Goyal *et al.*, 2000). Over this interval, binocular oscillations of OPT develop around all three axes (horizontal, vertical and torsional), and can be either conjugate or disconjugate (Deuschl *et al.*, 1994*a*; Leigh and Zee, 2006; Kim *et al.*, 2007). Interestingly, the eye movement waveforms are different in each patient, as opposed to say oscillations in vestibular nystagmus, in which the waveforms are similar in each patient.

Tremor in OPT requires an oscillator (Deuschl *et al.*, 1994*a*), but its location is uncertain. Involvement of the inferior olive is considered likely because (i) it shows hypertrophy in most OPT patients; (ii) the cerebellar symptoms develop on the side opposite to the abnormal inferior olive (Lapresle, 1986; Deuschl *et al.*, 1994*a*); (iii) motor learning, a cerebellar function that relies on the inferior olive, is abnormal in patients with OPT (Deuschl *et al.*, 1996); (iv) the tremor frequency in OPT patients is ~1–3 Hz, which is in the range of the frequency of rhythmic synchronous discharge from inferior olive neurons (Thach, 1970; Manor *et al.*, 1997); (v) olivary hypertrophy precedes the appearance of palatal myoclonus (Yokota and Tsukagoshi, 1991) and (vi) inferior olive neurons gradually die off (Nishie *et al.*, 2002) and, in a few cases that were observed for many decades (Leigh and Zee, 2006; Kim *et al.*, 2007), the OPT can diminish or even die out.

Is the inferior olive really involved in OPT?

These findings suggest that the inferior olive plays a significant role in OPT. However, other studies have cast doubt on this conclusion. The muscles (palatal, extraocular) usually involved in OPT are of branchial arch origin. The cerebellum and inferior olive are somatotopically mapped but do not seem to favour branchiomeric musculature, thus Kane and Thach (1989) argued that palatal myoclonus was more likely to arise from lesions of the central tegmental tract that denervate the nucleus ambiguus. Correlations of shrinking inferior olive size at autopsy with continued clinical symptoms seem to imply that the inferior olive may not be involved in maintaining OPT (Nishie *et al.*, 2002). PET imaging after amelioration of OPT with clonazepam shows a reduction in cerebellar activity, but no decrease in inferior olive activity (Yakushiji *et al.*, 2006). Kim *et al.* (2007) proposed that central lesions that give rise to OPT may also affect other structures nearby, such as the neural integrators in the pontomedullary tegmentum or the caudal dorsal cap of the inferior olive. This would give rise to a vertical-torsional or horizontal pendular nystagmus, respectively, caused by integrator failure.

These experiments argue against the interpretation of the inferior olive as the sole source of OPT, but they do not offer an alternative mechanism that can explain many of the features of OPT, including its frequency of ~2 Hz, the variability of its waveform in different patients, its slow time course of development and its amelioration or disappearance after many years.

We recently used simulations to show that the inferior olive alone was insufficient to generate the waveforms observed in OPT, and that amplification by the cerebellum was also required (Hong *et al.*, 2008*a*). Here we show that the confounding experiments (above) can be explained by the recent model of OPT as the result of dual inferior olive and cerebellar mechanisms. We compare the results of recordings from 15 OPT patients with simulations of that model, and investigate the relative importance of the inferior olive and cerebellum for OPT waveforms. The goal of this study was to show that most of the characteristics of OPT can be explained by the dual-mechanism hypothesis, and to show how drugs targeted at either the cerebellum or the inferior olive nuclei might affect OPT.

Dual-mechanism hypothesis

De Zeeuw and colleagues (1998) found that the synchronous inferior olive discharge after hypertrophy was periodic and jerky. Therefore, eye oscillations should also be periodic and jerky. However, ocular oscillations in OPT are aperiodic and smooth (Gresty *et al.*, 1982; Nakada and Kwee, 1986; Averbuch-Heller *et al.*, 1995; Kim *et al.*, 2007). These observations motivated an alternative idea, the dual-mechanism hypothesis (requiring both inferior olive and cerebellar mechanisms), to explain OPT (Liao *et al.*, 2008; Hong *et al.*, 2008*a*). Synchronized inferior olive oscillations and superimposed 'smoothing' due to cerebellar plasticity are central to this hypothesis. Below, we outline the physiological bases of both phenomena.

Inferior olive neuron characteristics

Normal inferior olive neurons share subthreshold membrane oscillations because they are electrotonically coupled via dendro-dendritic gap junctions formed by pre- and post-synaptic connexons (Fig. 1B, DD) (Llinas *et al.*, 1974; Sotelo *et al.*, 1974; Manor *et al.*, 1997; De Zeeuw *et al.*, 2003). Action potentials from inferior olive neurons travel up climbing fibres and give rise to complex spikes in the Purkinje cells of the cerebellar cortex. Climbing fibres branch and project to the deep cerebellar nuclei. Individual inferior olive neurons *in vitro* respond best to current injections with frequencies of 3–6 or 9–12 Hz (Llinas and Yarom, 1986). These experiments also showed that inferior olive neurons in a tissue slice can oscillate spontaneously at either ~6 or ~10 Hz, and some neurons in the slice have synchronous subthreshold oscillations at 4–6 Hz (Llinas and Yarom, 1986). The inferior olive neurons are grouped into 3D patches by their electrotonic coupling, which give rise to synchronous activity of complex spikes on groups of Purkinje cells (Llinas, 2009). However, *in vivo* these complex spikes do not appear to show synchronous oscillations related to movement in normal animals (Keating and Thach, 1995, 1997; Hakimian *et al.*, 2008). In our model, the output of

the inferior olive is a low level, random train of pulses from small patches, but in the normal condition these do not cause oscillations in the cerebellum or the extraocular muscles (Hong *et al.*, 2008*b*).

Lesions that disrupt connections from the deep cerebellar nuclei to the inferior olive remove GABA-mediated inhibitory modulation of these junctions (note that portions of the vestibular nuclei are essentially a displaced deep cerebellar nucleus for the vestibular cerebellum) (Sotelo, 1986). Over time the inferior olive nuclei undergo hypertrophy and abnormal soma-somatic gap junctions develop between adjacent neurons, which increases the strength of their electrotonic coupling (Fig. 1B, SS) (De Zeeuw *et al.*, 1990; Ruigrok *et al.*, 1990; De Zeeuw *et al.*, 1998; Bengtsson *et al.*, 2004).

When the coupling among neurons becomes strong enough, the oscillations of many cells can become synchronized, i.e. when one cell fires, many cells within its neighbourhood will also fire. As the strength of the electrical coupling increases, the size of that neighbourhood increases. Thus, the output of the inferior olive consists of random discharges from separate groups, or patches, of neurons. Neurons within a patch fire almost synchronously (in our model, all the cells within a patch fire within 4–10 ms of each other, depending upon the size of the patch), but patches discharge at random (see online supplementary movies showing the effects of normal, partial and complete coupling). Although the effect of synchronous firing of neurons in a normal-sized patch is too small to observe in an eye movement, the synchronous firing of neurons within an abnormally large patch could be large enough to cause movement (*cf*. Fig. 1C).

Cerebellar smoothing

The dual mechanism hypothesis stems from a computational study of the role of the cerebellum in generating learned timing (i.e. delay) in classical delay conditioning (Hong and Optican, 2008). In this hypothesis, the hypertrophy of the inferior olive leads to synchronous discharge within patches of electrotonically coupled neurons, each forming an independent, ~2 Hz pulsatile oscillator (Fig. 1C). The oscillator output is smoothed by the cerebellum, which learns to pause at the expected time of the next inferior olive pulse. Thus, a large number of cerebellar neurons, each with a slightly different delay (distributed around the expected delay of the inferior olive pulse), all pause creating a smooth output from the deep cerebellar nuclei (or vestibular nuclei, Fig. 1D). The output waveform from the combination of the olivary and cerebellar outputs is thus larger, smoother and less periodic than would be expected from the inferior olive output alone. Note that good visual acuity requires low retinal slip (~4°/s, Westheimer and McKee, 1975). Thus, the effects of cerebellar plasticity in OPT may actually be maladaptive for vision, as cerebellar plasticity causes movements that are actually two to three times faster than the smaller—but more jerky—movements without plasticity (in our model, eye velocity had a mean of ~0 and a standard deviation of ~17 and 6°/s, respectively).

Methods

Experiments were performed in two laboratories using the same procedures. The experimental protocol was approved by the ethics committees at both the Johns Hopkins and Case Western Reserve Universities. Eye movements were recorded from 15 OPT patients who had signed an informed consent document. In nine patients, MRI scans were performed after development of OPT; all nine showed inferior olive hypertrophy (Table 1). The protocols adhered to the Declaration of Helsinki for research involving human patients. See online supplementary data for further details on methods.

Search coil recordings

Three-dimensional binocular recordings were performed with dual search coils (Skalar Instruments, Delft, The Netherlands). Eye positions and velocities were represented as 3D rotation vectors in a head-fixed coordinate system.

Frequency measurement

The frequency content of the data from each patient (or simulated trial) was analysed by high resolution, modern spectral analysis (eigenvector method). This allowed us to characterize OPT waveforms in terms of their low frequency components.

Statistical analyses

MATLAB® tools were used for all analyses. Statistical independence was tested with independent component analysis (ICA) carried out with the fastICA package for MATLAB® (version 2.5, by Gävert, Hurri, Särelä, and Hyvärinen, Laboratory of Information and Computer Science, Helsinki University of Technology M).

Description of model

A model of classical delay conditioning (Hong and Optican, 2008) was modified (Hong *et al.*, 2008*a*) to examine the hypothetical mechanism of OPT. A simplified illustration of the model is shown in Fig. 1C. The structure of the model was divided into several modules.

Inferior olive module

This module (see supplementary data for more details) included the inferior olive and its anatomical connections (blue dashed line box in Fig. 1C). The module had left and right inferior olive nuclei. Each inferior olive neuron connected to its neighbouring neurons through gap junctions (zigzag lines in Fig. 1C and D). The equations summarizing the membrane properties of each of these units are provided in the supplementary material and in Hong and Optican (2008). The model inferior olive projected contralaterally to the vestibular nuclei, which projected to the oculomotor nuclei (Balaban, 1988). The effects of inferior olivary hypertrophy were simulated by gradually increasing the electrotonic coupling between neighbouring inferior olive neurons (De Zeeuw *et al.*, 1990; Ruigrok *et al.*, 1990).

Cerebellar module

The inferior olive output reaches the Purkinje cells through climbing fibres (direct inferior olive to Purkinje cell connection) and via parallel fibres (an indirect signal via vestibular nuclei and granule cells) (Zhang *et al.*, 1993). This circuit is represented in Module 2 (green dashed line box in Fig. 1C). Figure 1C and D show the circuit carrying these two

Table 1 Patient clinical highlights

Patient	Age/sex	Diagnosis	Duration/delay	Medicines
P1	25/M	Haemorrhage from pontomedullary arteriovenous malformation	2 years/6 months	None
P2	37/M	Haemorrhage from pontine arteriovenous malformation	2 years/1 month	Verapamil
P3	53/M	Brainstem haemorrhage from pontine arteriovenous malformation	2 years/6 months	Baclofen pump
P4	34/F	Basilar occlusion, pontine infarction	18 months/1 week	None
P5	48/M	Brainstem haemorrhage from pontine-mesencephalic vascular malformation; MRI: increased inferior olive signal	10 months/1 month	Clonazepam, Memantine
P6	57/M	Pontine infarction, MRI: increased inferior olive signal	18 months/38 months	None
P7	52/M	Posterior fossa choroid plexus papilloma removal, cerebellar infarction; MRI: increased inferior olive signal	10 months/4 months	None
P8	45/M	Pontine haemorrhage, cavernoma; MRI: increased inferior olive signal	1 month/11 months	Levodopa/carbidopa, Amlodipine, and Beta-blocker
P9	46/F	MRI: enlarged inferior olive	42 months (duration)	Gabapentin, Atenolol
P10	41/F	Palatal tremor developed one year after labyrinthectomy for recurrent vertigo, MRI: left inferior olive hypertrophy	5 years (duration)	Fluoxetine, Trazadone
P11	61/F	MRI: right inferior olive hypertrophy; no palatal tremor	3 months	None
P12	57/M	Head injury; bifrontal and occipital contusions with subarachnoid bleed	1 year	Terazosin
P13	57/F	Benign cerebellar tumour excised at age 6 year	6 years	Pregabalin, Duloxetine, Diazepam
P14	30/F	Pontine haemorrhage, MRI: inferior olive hypertrophy	18 months	None
P15	37/M	Pontine OPT following R > L pons haemorrhage, palate involved, MRI: right inferior olive hypertrophy	16 months	Lisinopril, Labetalol, Hydralazine, Nifedipine

signals; only one Purkinje cell and interneuron pair is shown for simplicity. This aspect of the model led to periodic climbing fibre and parallel fibre inputs to PC–interneuron pairs at approximately the same time. This simulation features the effects of the periodic conjunction of the parallel fibre–climbing fibre signals to train the parallel fibre–interneuron pairs. After learning, Purkinje cells can pause after the parallel fibre input at the time of the next expected climbing fibre input. Thus the Purkinje cells oscillate with the ongoing inferior olive pulses, which modulate the activity relayed through the vestibular nuclei. This form of learning and execution, without parallel fibre long-term depolarization, emphasizes the role of vestibular nuclei–inferior olive circuit as demonstrated by the persistence of vestibular adaptation even without cerebellar long-term depolarization (Faulstich *et al.*, 2006). Cerebellar timing without Purkinje cell long-term depolarization has also been described by Welsh *et al*. (2005). The equations corresponding to the cerebellar learning are described in Hong and Optican (2008).

Eye plant module

Eye movements were simulated using a three-axis, first-order ocular motor plant for each eye (Robinson, 1982). Mathematical details are provided in the online supplementary information.

Results

Figure 2 shows 3 s epochs of horizontal, vertical and torsional eye positions of both eyes from 15 OPT patients. Qualitatively, these traces appear irregular in shape, aperiodic, smooth and distinct from one another. Within a given patient, the traces could appear conjugate, i.e. symmetric in both eyes (Patients 1–3, 5, 9, 15) or asymmetric (Patients 6–8, 10–14). Note that Patient 4 had only two eye recording channels. Symmetry may be important when characterizing the degree of inferior olive hypertrophy on a spectrum from uni- to bi-lateral, although Kim *et al*. (2007) did not find this to be a strict correspondence.

Frequency components

Figure 3 shows the power spectra of the oscillations for each patient for both eyes and each axis. In some patients there was a unique sinusoidal component (e.g. Patients 1, 2, 5, 6, 7, 10) that was the same in both eyes and around each axis. In the other patients, there could be two or more large components and these could be different around different axes, although they were usually similar (symmetric) in the two eyes. Table 2 shows the range of sinusoidal components found near each frequency from 1 to 3 Hz.

Figure 4 shows the weighted average frequency of the dominant spectral peak (i.e. peak with highest power between 1 and 5 Hz). We can infer from the result in Fig. 4 that the oscillation mechanism in each patient is very robust, because the frequency range (SD bars) is very small (< ~10%). We infer from this that the frequency of oscillation is determined by a basic membrane property of the neurons and not the properties of a closed-loop circuit. In a multi-element circuit, the phase lag through each

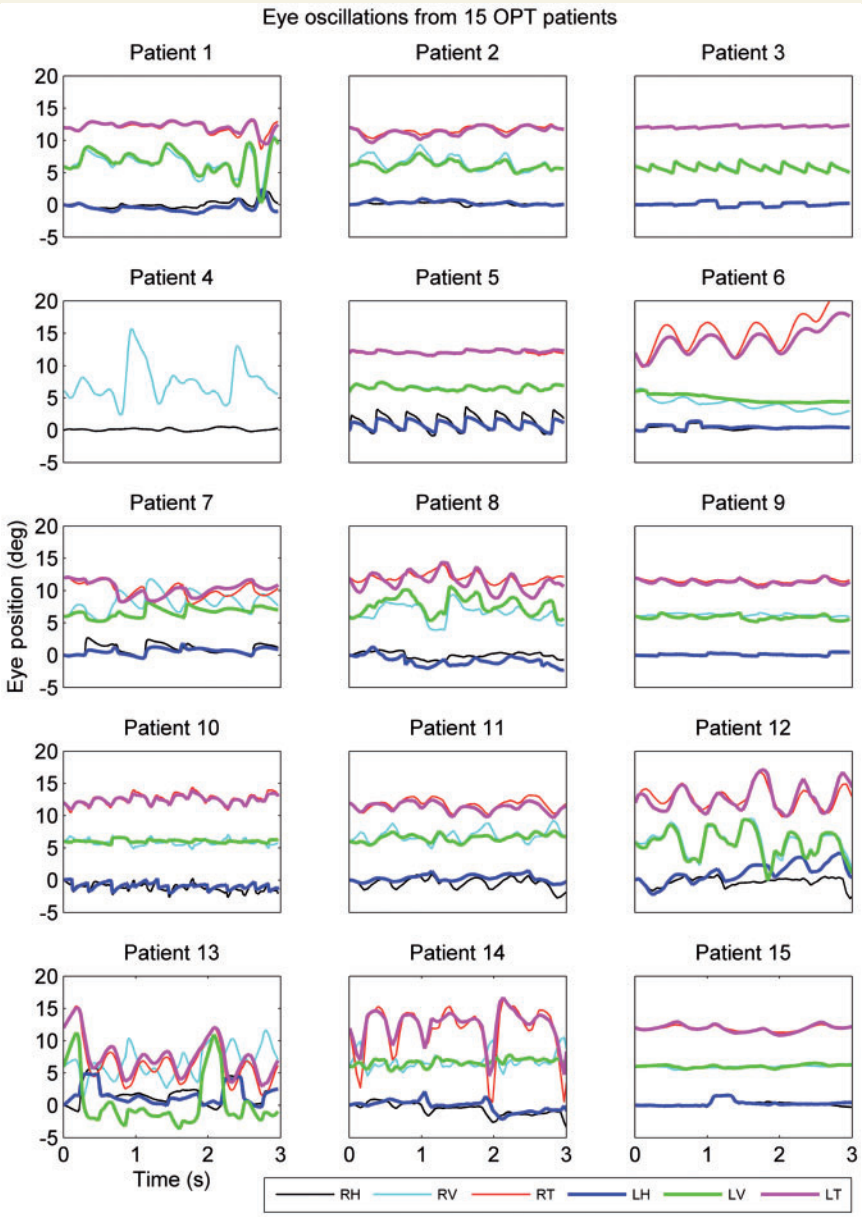

Figure 2 Three second epochs from records of binocular recordings from 15 OPT patients. Three-axis movements (H = horizontal; V = vertical; T = torsional) of the right (R) eye (thin lines) and left (L) eye (thick lines) are plotted (see legend for colors). In some patients (e.g. Patient 3) the movements are conjugate (symmetric). In others (e.g. Patient 8), they are disconjugate (asymmetric). Note the variability of qualitative features of the waveforms between patients.

element and the time delay around the closed loop, determine the frequency of oscillation. One might expect these to drift with factors such as attention, thereby changing the frequency, whereas membrane conductances (such as the repolarization currents in the soma) would presumably be less affected by such changes. If the oscillator were formed from a closed-loop circuit, the frequencies would be expected to cover a wider range. In contrast, the range of membrane properties should be more constrained, as presumably different frequencies correspond to membrane proteins that come from slightly different genes. In the set of patients in Fig. 4 we see less than a 3-fold variation in frequency, which is quite close to the range seen in zebra fish heart rate with defective pacemaker currents because of mutated I_h channel proteins (Baker *et al.*, 1997).

Independent generators

Although we recorded six components of our eye movement signals, it is possible that these eye movements are the output from a smaller number of internal generators. For example, there could be only one generator that is distributed to each agonist–antagonist muscle pair. The signals we record could then look different just because they are corrupted by noise, or the OPT lesion may have differentially affected other premotor structures important for eye

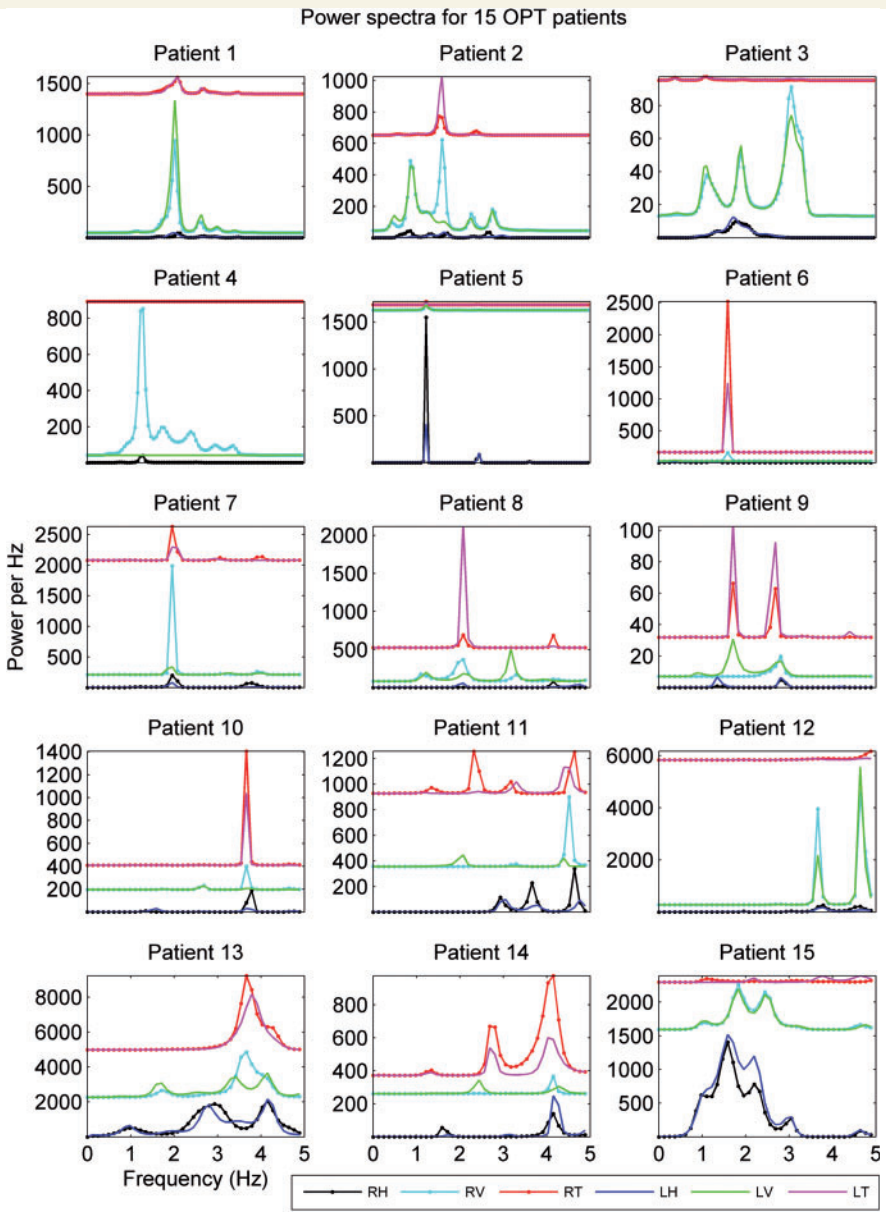

Figure 3 Power spectra from the same 15 OPT patients (H = horizontal; V = vertical; T = torsional). Entire record during fixation straight ahead, sampled at 500 (Patients 1–5) or 1000 Hz (Patients 6–15) was used to obtain a very high resolution ($\Delta F = 0.0610$ or 0.1221 Hz, respectively) spectrum. Duration of records ranged from 3 to 120 s across patients. Only the low frequency components (0–5 Hz) are shown because higher frequencies are not relevant for characterizing OPT waveforms. In different patients the spectra can be the same, or different, for movement around different axes. Note that pairs of spectra (for right and left eyes) have been arbitrarily offset along the ordinate for clarity (see legend for colors).

Table 2 Weighted average frequencies of sinusoidal components in 0.5 Hz bands across all OPT patients

Centre frequency of band (Hz)	Mean (Hz)	SD	Number of patients
1	1.16	0.17	13
1.5	1.55	0.23	14
2	1.93	0.25	15
2.5	2.58	0.29	14
3	2.93	0.20	14

movements (Leigh and Zee, 2006; Kim *et al.*, 2007). Alternatively, there may be three generators, say for horizontal, vertical and torsional movements, but they are sent as conjugate signals to both eyes. Again, noise might make these signals look different. If the noise is Gaussian and additive (i.e. not modulatory or multiplicative), we can determine the number of independent generators with an ICA. ICA separates multiple signals into additive subcomponents that are statistically independent (see online supplementary information for an intuitive explanation of ICA). In the first example given above, ICA would find one generator signal

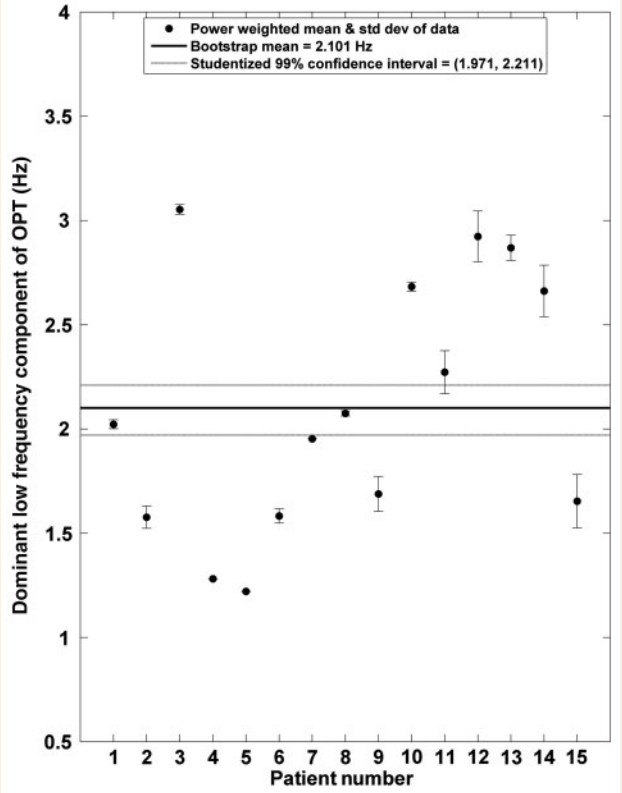

Figure 4 Quantitative summary of the dominant frequency of OPT oscillations in each patient. As shown in Fig. 3, each patient had a different pattern of oscillations that could be characterized by a few low frequency components. In this plot, the weighted average frequency of the largest peak in the power spectrum across both eyes and all three axes is shown. Each dot is the mean of the peak from each eye and axis, weighted by the power contributed by that peak (error bars show weighted SD). The bootstrap method (with 10 000 resamplings) was used to estimate the mean and SD from all 15 patients (horizontal lines). The bootstrap mean of the patients' dominant spectral component was 2.101 Hz (studentized 99% CI was from 1.971 to 2.211 Hz).

and one noise source (it doesn't differentiate among different sources of Gaussian noise). In the second example, ICA would find three subcomponents and one noise component. As schematized in Fig. 5A, if a given set of output signals (red waveforms) were a mixture (light grey box) of six independent oscillators, the ICA algorithm (grey arrow) would find six independent signals (green) and reveal how the output signals share the input signals. ICA in each OPT patient revealed six independent sources in all patients (Fig. 5A). ICA in each run of the model (see below) also revealed six independent sources (Fig. 5B). Note that the ICA algorithm cannot find more sources than there are mixture signals to process.

These results make it unlikely that OPT is caused by a small number of oscillators in the inferior olive. A simple explanation is that there are multiple, independent oscillators in the inferior olive. This is a reasonable assumption, because a hypertrophic inferior olive with increased electrotonic coupling would probably not synchronize all the cells in the inferior olive into a single group. Rather, it would seem more likely that only neurons within a small patch would fire together. However, many such small patches would be firing independently. The activity coming from the cerebellum would also correspond to independent patches, each trying to predict the arrival of an input pulse from an inferior olive patch. Thus, it would appear as if synchronous activity were occurring within many random patches of inferior olive and cerebellum.

The idea that small patches of cells in the inferior olive and cerebellum are firing randomly may also explain why the waveforms in OPT patients seem so different. Each patch would be connected to a different part of the motor system, and thus some patches would give rise to horizontal movements and others to vertical or torsional movements. Indeed, some patches would presumably project to other muscles (see below). If the distribution of conductance increases in the inferior olive was not uniform, and it was different in each patient, different patients would present with different waveforms. The lesion may also affect other parts of the brain (Kim *et al.*, 2007), causing the OPT waveform to be the sum of different waveforms from inferior olive, cerebellum and brain stem sources.

Ocular oscillations caused by inferior olive synchrony alone

Ocular oscillations in OPT might simply be generated by synchronous activity within the hypertrophied inferior olive alone (De Zeeuw *et al.*, 1990; Ruigrok *et al.*, 1990; De Zeeuw *et al.*, 1998; Bengtsson *et al.*, 2004). We tested this hypothesis in our distributed model by simulating the effects of increased gap junctions in the inferior olive module, but without cerebellar plasticity (Fig. 1C). This simulation showed synchronized spiking activity among neighbouring inferior olive neurons. During simulation, the inferior olive activity seems to start randomly at different locations (see Supplementary Fig. 4 for a spike raster plot and supplementary movie clips for animated activity maps; see also Hong *et al.*, 2008, Fig. 3).

This activity is consistent with our prediction that synchronous activity occurs within random patches of inferior olive and further excludes the possibility that OPT is caused by a single oscillator. The resulting inferior olive output consisted of narrow, periodic bursts of activity (black inferior olive/climbing fibre traces Fig. 1C). These periodic spikes then propagate to the eye muscles via the vestibular and brainstem oculomotor nuclei. The effects of synchronized inferior olive firing on eye movements manifested as ~2 Hz, small, regular and jerky eye oscillations (magenta trace at the bottom of Fig. 1C). Note that although the frequency is similar (~2 Hz), the simulated eye oscillations in Fig. 1C do not look like the traces from patients, which are bigger and more irregular (Fig. 2).

Post-processing of inferior olive discharge

If there were a single oscillator in the inferior olive, one could explain the unique shape of each oscillatory waveform in a given patient by proposing that the inferior olive generated signal undergoes some form of post-processing (e.g. low-pass

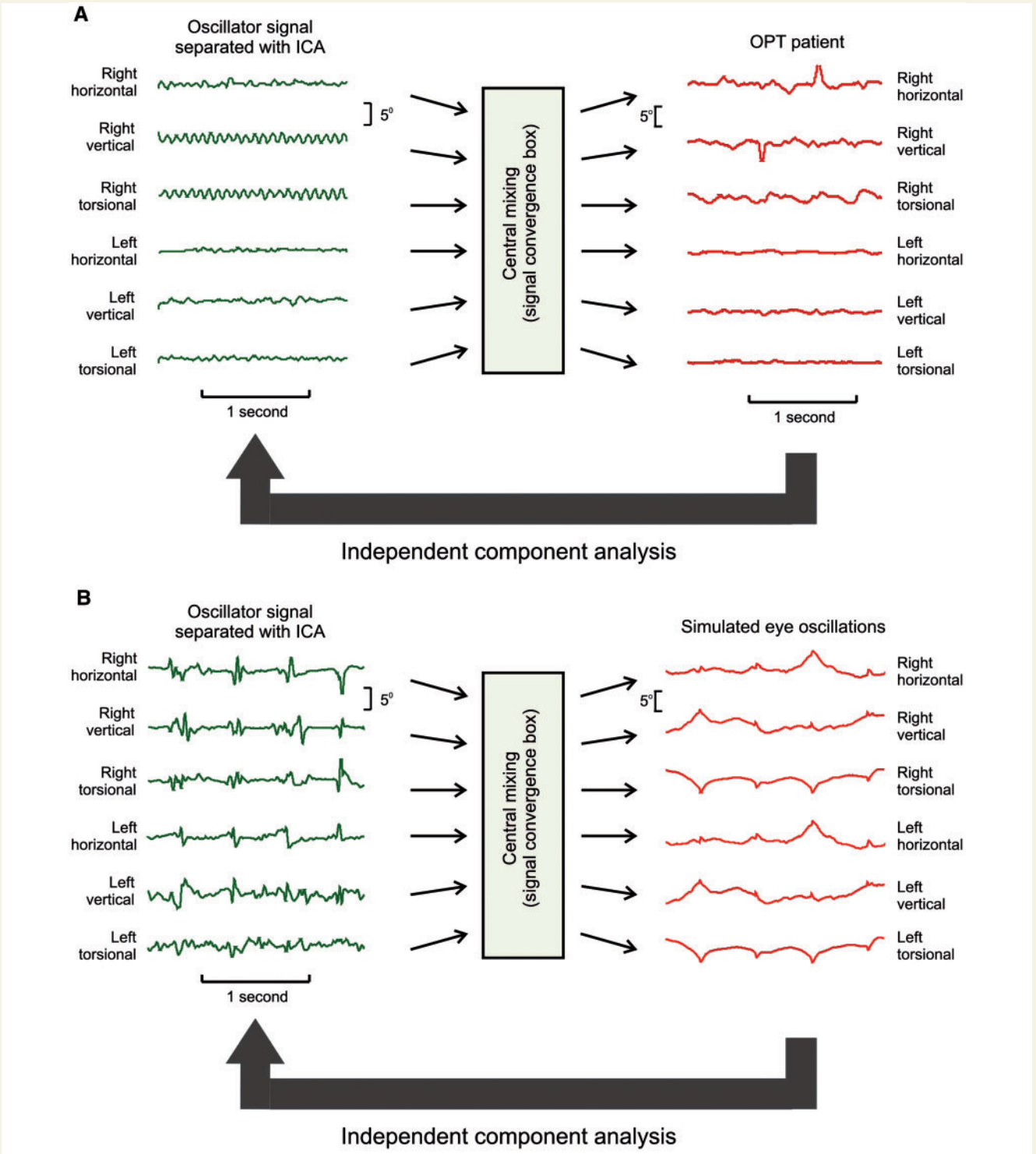

Figure 5 Schematic showing the principle of ICA. A given set of observed, mixture signals (red oscillations) are presumed to be a linear mixture (central box; hypothetically the vestibular or deep cerebellar nuclei) of six hidden, independent oscillators (green waveforms). The ICA algorithm (grey arrow) would find at most six independent signals and reveal how they are mixed to form the output signals. Examples of this analysis from one patient (**A**) and one simulation run (**B**) are illustrated.

filtering or adding noise). This proposal, however, predicts that the shapes of the waveforms would look like the impulse response of a filter, i.e. delayed relative to the peak of activity (presumably from the inferior olive pulse). In other words, a sharp, symmetrical peak would become smeared to the right. To look for such a rightward skewing of the eye movement waveform we aligned a sharp, symmetric, peaked waveform (to represent the inferior olive output pulse) with the peak of each cycle of the ocular oscillation, and subtracted it from the waveform (Fig. 6).

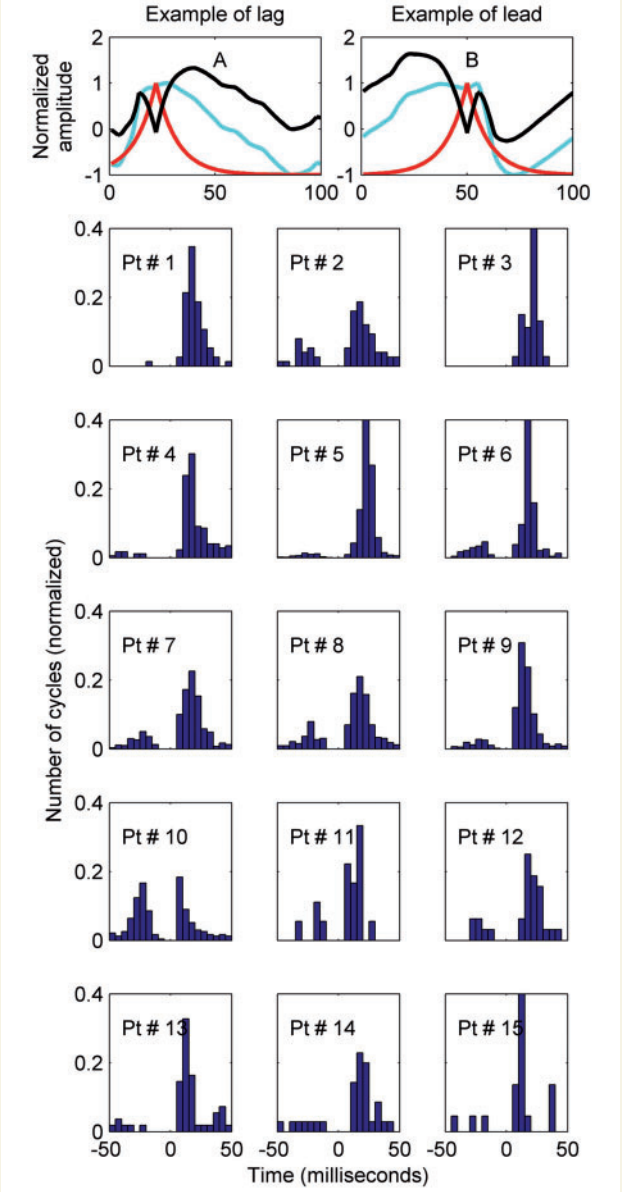

Figure 6 An example of cycles where the residual signal (black trace), i.e. the difference of the actual signal (cyan trace) and presumed inferior olive spike (red trace) lagged (**A**) or led (**B**) the peak of the inferior olive spike. The histograms in the lower part of the figure show the distribution of the time differences between the peak of the inferior olive pulse and the peak of the residual signal for each patient (Pt). A positive value of the time difference indicates that the residual signal lags the inferior olive pulse and a negative value represents a lead. If the eye movement waveform were the result of post-processing the inferior olive pulse, one would expect to see the residuals lag the pulse. However, in several patients (e.g. Patients 2, 8 and 10) the waveform leads the inferior olive pulse.

The residual signal represented the effect of downstream filtering on the inferior olive output. Light blue traces in Fig. 6A and B illustrate examples of representative cycles of the recorded oscillation. The red traces represent the putative inferior olive output pulse. The black traces show the residual signal. Note that in Fig. 6A most of the area under the black trace is after the inferior olive pulse, whereas in Fig. 6B, for the black trace, most of the area is before the inferior olive pulse. The histograms in the lower part of Fig. 6 show the distribution of the time differences between the peaks of the inferior olive pulse and the peaks of the residual signal. In some patients most of the residual peaks lag the inferior olive pulse, but in others (Patients 2, 6–10) there are a large number of cycles where the residual peak leads the inferior olive pulse. If post-processing of an inferior olive oscillator introduces irregularity in the eye movement waveform, the peak of the residual signal should always lag the peak of the inferior olive signal. Hence, these data are inconsistent with the hypothesis that the waveform irregularity of OPT oscillations reflects post-processing of a signal generated by the inferior olive alone.

Ocular oscillations caused by both inferior olive and cerebellum

According to our hypothesis, the hypertrophic inferior olive generates regular, pulsatile oscillations (Fig. 1C) and the cerebellum learns to contribute a smoothing and amplifying pulse (Fig. 1D). The inferior olive output goes both to the vestibular nuclei and to the cerebellum, via climbing fibres (Andersson and Oscarsson, 1978). inferior olive activity thus reaches the cerebellar cortex by two routes, directly on the climbing fibres, and indirectly via the climbing fibre collaterals that go to the vestibular nuclei, which in turn provide mossy fibre inputs to the cerebellum (Carpenter *et al.*, 1972). The mossy fibres thus carry an inferior olive signal via the parallel fibres to the cerebellar cortex. The periodic conjunction of the first inferior olive pulse arriving via the parallel fibres and the next inferior olive pulse arriving via the climbing fibres can manifest as an anticipatory pause of the Purkinje cell at the expected time of the next inferior olive pulse (i.e. classical delayed conditioning in response to an inferior olive pulse). Hence, the output of the cerebellum (dark green traces in Fig. 1D) will not be synchronous with the average inferior olive output (black traces in Fig. 1D) going to the eyes, but could be either earlier or later. The Purkinje cell pause modulates the activity of the vestibular nuclei, resulting in an eye movement waveform (magenta trace, bottom of Fig. 1D) that is larger and more irregular than an inferior olive signal itself would produce (magenta trace at bottom of Fig. 1C). Note that, according to this hypothesis, the Purkinje cell output is predicting the next inferior olive pulse. Thus, the Purkinje cell output is asynchronous with the inferior olive pulses, and therefore may either lead or lag the inferior olive discharge. This is consistent with the analysis above (Fig. 6).

We further tested this hypothesis by simulating the learning effect of Purkinje cells on the target vestibular nuclei neuron (Module 2 and online supplementary data). Figure 7 illustrates simulated three-axis, binocular eye movements after inferior olive hypertrophy and cerebellar learning in 15 independent simulations. Figure 8 shows the power spectra for these simulations.

The simulated oscillations were irregular, smooth and the frequency in 15 *de novo* simulation trials was always close to 2 Hz. The model attributes the uniqueness of the waveforms to the

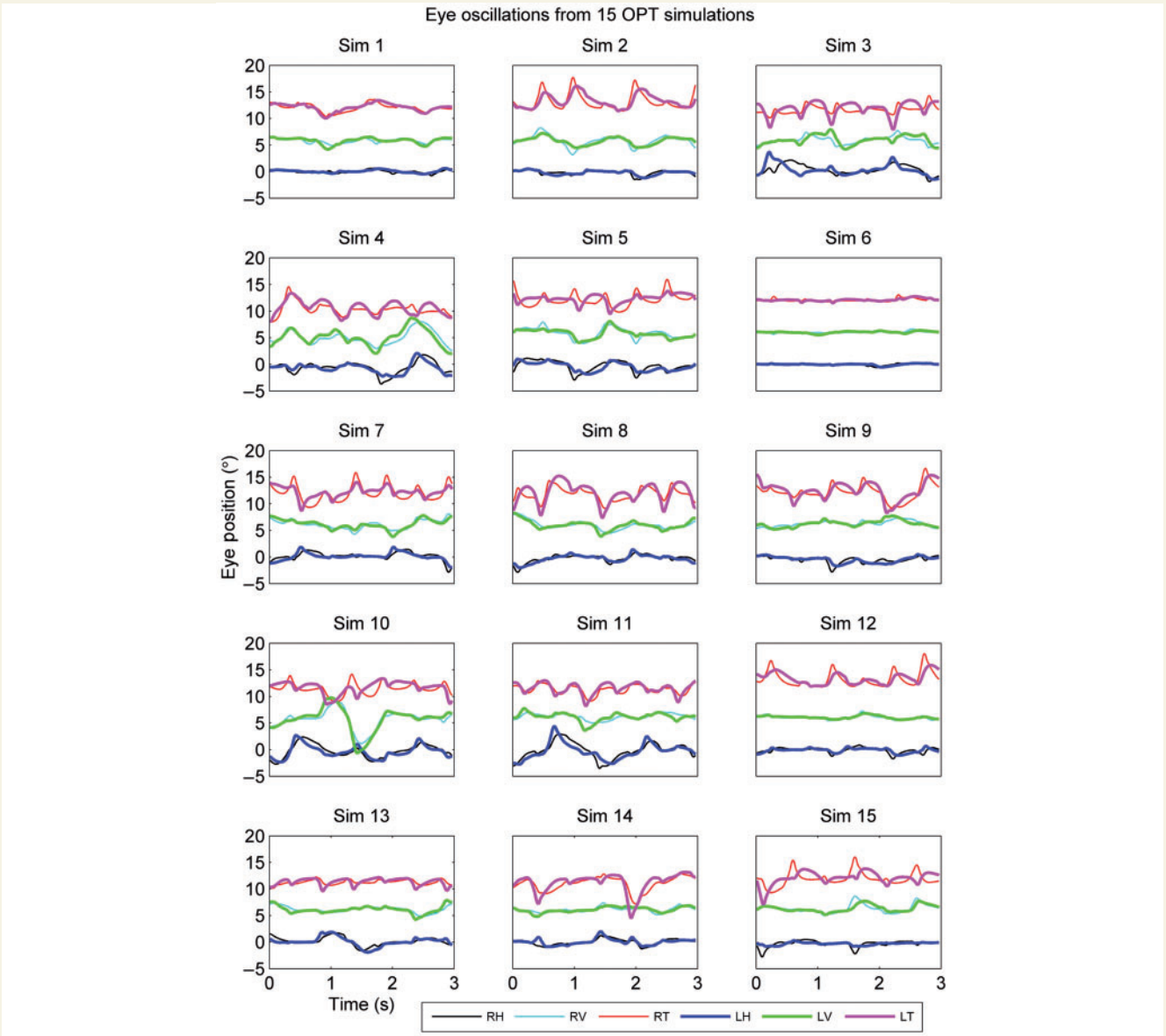

Figure 7 The qualitative illustration of 3D oscillations generated by 15 *de novo* model simulations (same format as Fig. 2; see legend for colors). Each panel shows a 3 s epoch of simulated 3D eye movements. It is emphasized that during each of the 15 simulations, the model started from random initial values and suffered a lesion distributed randomly through the inferior olive. Note that the qualitative features of oscillations were different in different runs, although not as strikingly different as the range of waveforms seen in OPT patients (Fig. 2).

variability in the distribution of activity within the inferior olive, and the smoothing by the cerebellum. This hypothesis also emphasizes that the coupling of large climbing and parallel fibre signals from the inferior olive is a pathological phenomenon. Such phenomena are secondary to the abnormally enhanced gap junctions synchronizing the discharge of many inferior olive neurons. Under normal conditions, the same model with unsynchronized inferior olive neurons does not generate synchronous, periodic pulses (Hong and Optican, 2008). This fact is demonstrated in Supplementary Fig. 4 and the Supplementary movie clips.

Comparing Figs 8 and 3 also shows that there is a much narrower range of dominant frequencies in the simulations than in our set of patients. The main reason for this is that the simulations all used the same equations for the inferior olive neurons, and therefore all their repolarization currents followed the same time course. Thus, in most cases the frequency of oscillation was almost exactly 2 Hz. Nonetheless, in a few runs (e.g. 1, 6, 9, 13 and 14) there were major contributions by other frequencies around some axes, usually at ~0.8 or 4 Hz. These must have arisen from randomly formed couplings within the inferior olive modules, as these other frequencies were often unique to one or a few axes and eyes. This suggests one possible mechanism for the range of frequencies seen around different axes within the same patient (Fig. 3, Patients 2 and 12). Another mechanism would simply be inter-individual variability in gene expression profile of the ion channel proteins in inferior olive neurons, giving them different time constants.

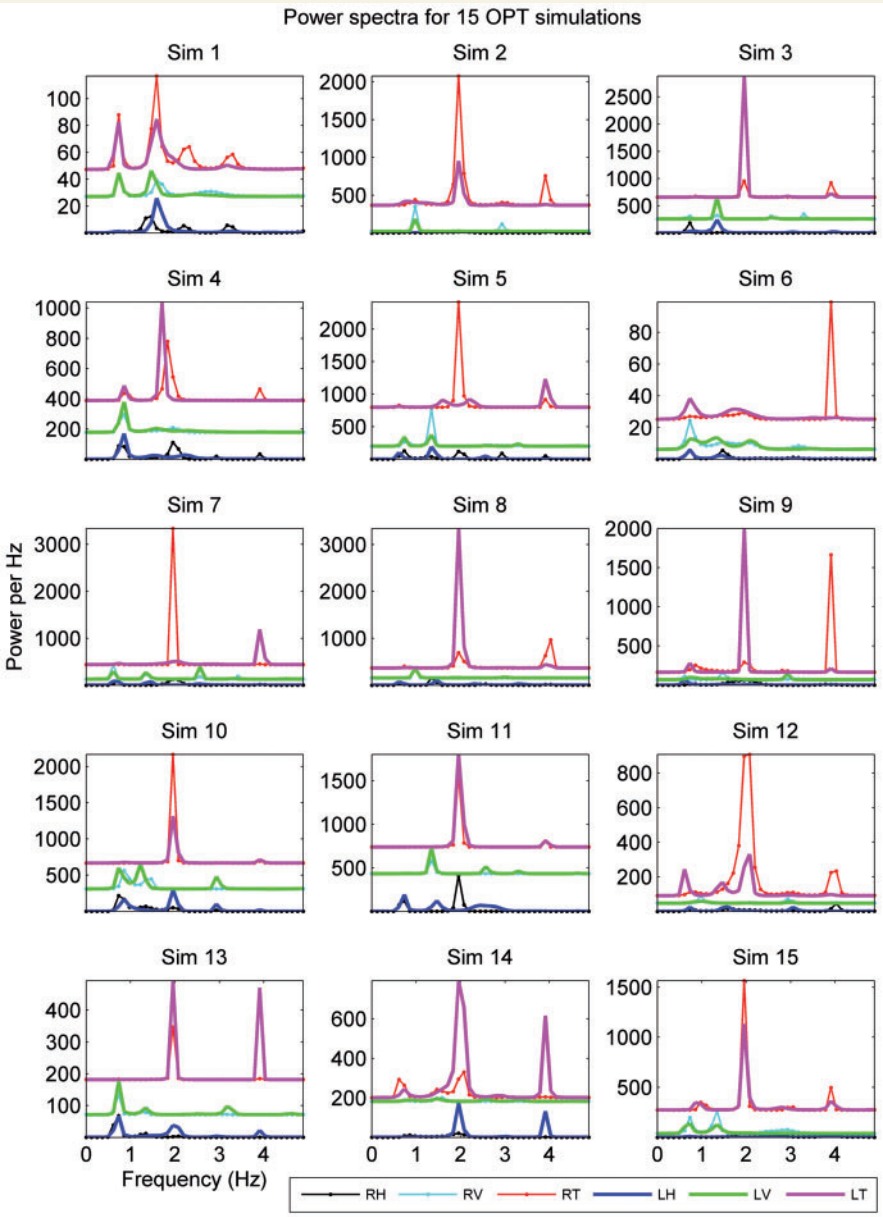

Figure 8 Power spectra from the same 15 simulations (format is the same as Fig. 3; see legend for colors). Entire record (20 s), sampled at 1000 Hz, was used to obtain a very high resolution ($\Delta F = 0.1221$ Hz) spectrum. For different simulations the spectra can be the same, or different, for movement around different axes. Note that when the dominant frequency was very high (above about 3 Hz), the amplitude of the oscillation (Fig. 7) and thus the power per Hz (note ordinate scale), was very small (e.g. simulation 6). Note that pairs of spectra (right and left eyes) have been arbitrarily offset along the ordinate for clarity.

Note that the 15 runs were not intended to simulate any particular patient's records. Rather, they show that the model produces waveforms that are not the same on each run, i.e. they are idiosyncratic to the randomly assigned effects of the lesion. Nonetheless, the statistical properties and power spectra of movements found in the 15 simulation runs are similar to those of the 15 patients.

It is clear from comparing Figs 7 and 8 with Figs 2 and 3 that the detailed shapes of the simulated waveforms match only a few of the patients' waveforms. One reason for this is shown in Fig. 9, where simulations were run with gains of the lesion effects on the cerebellum or inferior olive of 20%, 40% and 80%. In these simulations the waveforms change considerably, suggesting that to model the waveforms of a specific patient we would have to tune the strength of the cerebellar output and the degree of inferior olive synchronization appropriately. Furthermore, as noted above, other areas affected by the lesions causing OPT may affect the waveforms, which could not be simulated in this model. For example, in Fig. 2, Patients 3 and 5 seem to have a jerk nystagmus and Patient 6 seems to have a pendular nystagmus around one axis. These additional features may be due to damage to the vestibular system rather than inferior olive hypertrophy. Similar variations are seen in other studies of human patients and are usually ascribed to lesions that affect nearby structures (Kim *et al.*, 2007).

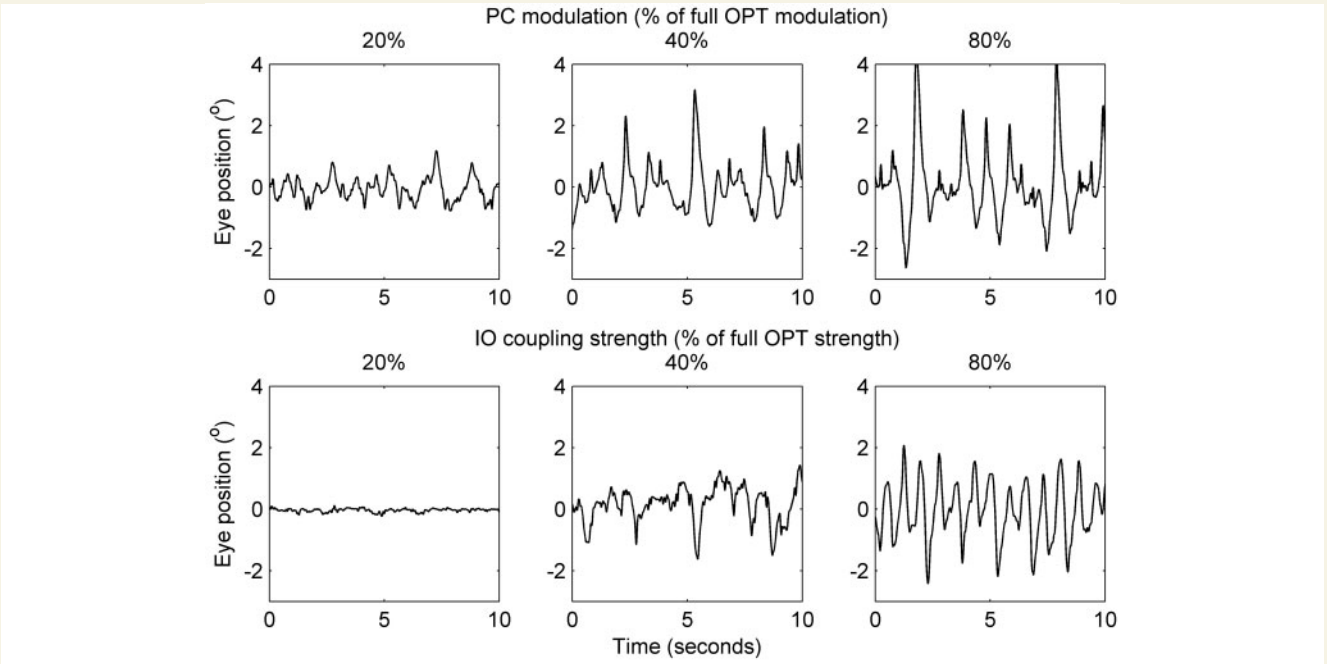

Figure 9 The effects of progressively reducing the contribution of cerebellar learning or inferior olive coupling on OPT. Top row shows effects of reducing the modulation of the deep cerebellar nuclei by Purkinje neurons (PC). The full modulation after learning for OPT would be 100%. The second row shows the effects of reducing coupling strength among inferior olive neurons. Full strength after hypertrophy in OPT would be 100%. Each record shows a 10 s epoch of the eye position record, chosen around the axis with the smallest variance.

Model predictions of drug effects on OPT

According to the dual-mechanism hypothesis, the large amplitude and smoothness of the OPT waveforms can be attributed to learning-induced responses from the cerebellum and the spiky ~2 Hz oscillations can be attributed to the synchronous inferior olive discharge. The model thus affords a way to make predictions about how different drugs might affect the oscillations in OPT patients. We simulated the model when the function of either the inferior olive or the cerebellum was altered, to indicate the range of behaviour that might be elicited by therapeutic treatments.

If the pause in Purkinje cell inhibition on vestibular nuclei neurons is reduced, the amplitude, smoothness and aperiodicity of the simulated waveforms should be reduced. Figure 9, top row, shows the effects of reducing Purkinje cell modulation of vestibular nuclei neurons (gains of 20, 40 and 80%). As the effect of the cerebellar learning becomes larger, the simulated waveforms become larger. Changing the gain of the inferior olive coupling to 20%, 40% or 80% of full strength caused the movements to grow from nothing to a moderately sized oscillation.

Figure 10 summarizes the effects of changing the gain of either the cerebellum (learning) or the inferior olive (coupling). In Fig. 10A we see that decreasing the effect of cerebellar learning to zero reduces, but does not stop, the oscillations. In contrast, reducing the gain of the inferior olive coupling to 20% completely stops the OPT oscillations. In Fig. 10B we see that the frequency of the oscillations is largely unaffected by the gains. That is because in the model the oscillation frequency is due to the time course of the repolarizing currents (e.g. delayed rectifier potassium and anomalous inward rectifier currents) of the inferior olive neurons (Schweighofer *et al.*, 1999, 2004; Hong and Optican, 2008), and not circuit properties that would depend on gains.

Discussion

The model used here simulated the role of the cerebellum in classical delay conditioning of the tone-puff blink reflex in animals (Schneiderman *et al.*, 1962; Hong and Optican, 2008). This dual-mechanism model emphasizes the pivotal role of increased soma-somatic gap junctions between inferior olive neurons (De Zeeuw *et al.*, 1990; Ruigrok *et al.*, 1990) in synchronizing inferior olive neurons and generating oscillations. However, the shape and amplitude of the waveforms are due to maladaptive plasticity of the cerebellum (Hong *et al.*, 2008*b*).

We emphasize that the model parameters were not adjusted to match the oscillations in particular OPT patients. Nonetheless, the model is sufficient to reproduce many of the effects of OPT, although it cannot prove that the inferior olive and cerebellum are necessary for OPT. The idea that the cerebellum is involved in OPT is novel, but the suggestion that the inferior olive is involved has long been controversial. We shall now discuss and attempt to refute some of the arguments against the hypothesis that the inferior olive is involved in OPT.

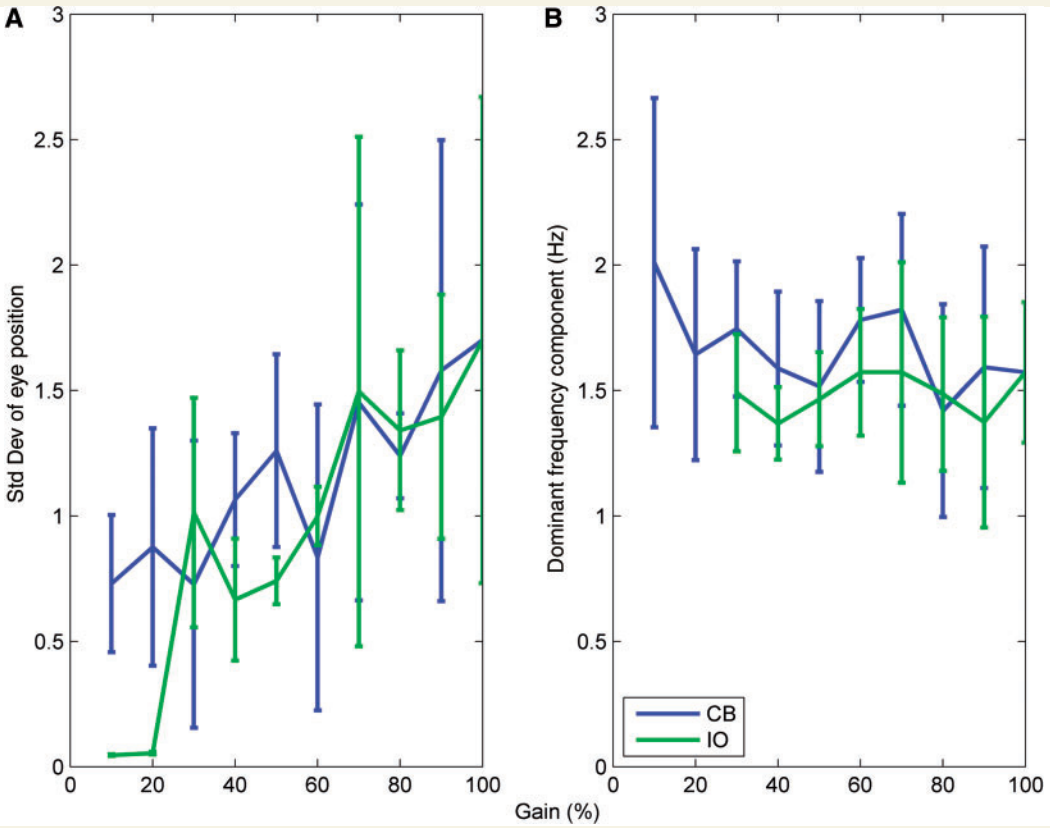

Figure 10 Progressively reducing the inferior olive coupling strength (green) or cerebellar modulation (blue) (gain is per cent of full strength) reduces amplitude but not frequency in simulated oscillations. (**A**) Increasing either cerebellar or inferior olive gain increases the amplitude of the oscillations (represented here by the standard deviation of the eye position traces). Note that when the inferior olive gain is below 30%, there are no oscillations. However, when the cerebellar gain is below 30%, oscillations persist. This is expected, because in the model the source of the oscillations is the train of random pulses from the inferior olive. (**B**) Changing the gain of either the cerebellum or inferior olive has little effect on the dominant frequency component of the oscillations. This is expected, because the frequency is determined by the repolarization currents in the inferior olive neurons, not by feedback circuits among the cells. Mean and SD come from averaging over 10 runs of one eye around three axes of rotation ($n = 30$).

Role for the inferior olive in OPT

Synchronous discharge from the hypertrophied inferior olive is the commonly proposed mechanism for OPT (Guillain and Mollaret, 1931; Matsuo and Ajax, 1979; Deuschl *et al.*, 1990). However, several studies have cast doubt on this mechanism. Below we consider the major arguments against the inferior olive as part of the mechanism for OPT.

Loss of inferior olive cells over time

Nishie and colleagues (2002) studied the morphology of the inferior olive in autopsy material from patients who had persistent OPT. In patients who died more than six years after their OPT developed, the number of inferior olive neurons was reduced by 90%. The authors concluded that OPT was initiated by hyperactivity in the hypertrophic inferior olive, but that some other mechanism must maintain the OPT. Their conclusion assumes that a larger than normal output of the hypertrophic inferior olive is responsible for the OPT oscillations. As some of the cells die off, the total output would be reduced, and the drive for the OPT would then have to come from somewhere else. However, in our theory, it is not the number or amount of hyperactivity of inferior olive neurons that causes oscillations. Instead, it is the increase in the strength of the electrotonic coupling between cells which causes them to oscillate synchronously. These oscillations, even if small, are then amplified by learning in the cerebellum. A reduction in the number of inferior olive neurons does not necessarily mean that the strength of the coupling between the remaining cells has been reduced. Thus, in our model, oscillations persist and are amplified by the cerebellum even after a large reduction in the number of cells in the inferior olive. However, as shown in Fig. 10, an 80% reduction of coupling strength among inferior olive neurons would stop the oscillations in our model. Thus, if inferior olive neurons continue to die off over time, oscillations would eventually cease. This is consistent with the amelioration of OPT seen in some patients after several decades.

Lack of inferior olive involvement in OPT treatment

A positron emission tomography (PET) study of one OPT patient showed increased glucose uptake in the inferior olive and the cerebellum (anterior vermis), but only the activity in the cerebellum

declined with clonazepam treatment (Yakushiji *et al.*, 2006). Our prediction that the inferior olive is the primary generator of the abnormal oscillation is consistent with these findings. Assuming clonazepam reduced cerebellar activity, the nystagmus would then be driven only by the inferior olive, and thus would be spikier and smaller (Fig. 1C and D).

OPT and movement timing

Kane and Thach (1989) argued against the inferior olive as the source of palatal myoclonus, although they did not consider the cause of the ocular oscillations in OPT (Deuschl *et al.*, 1994*a*, *b*). They tested two theories of inferior olive function. One was that the inferior olive acted as a ~10 Hz clock for initiating ballistic movements, and one that it was involved in motor learning. They ruled out both hypotheses by showing that there was not a significant difference in performance between two normal subjects and two subjects with palatal myoclonus. However, as noted below, others have reported that motor learning in patients with OPT is actually slower than normal. They inferred from this that the inferior olive could not be the cause of the palatal myoclonus. Importantly, their conclusions rested on the key assumption that all of the olivary cells 'are slavishly synchronized and firing at a uniform rate of 1–2 Hz' and during learning 'individual olive cells must fire singly in relation to the stimulus responses to accomplish the adaptation'. As shown by our model, 100% synchronization is not required for OPT. Furthermore, different muscles are involved in symptomatic and essential palatal tremor (see below). Thus, their conclusion that the inferior olive could not be causing myoclonus does not necessarily rule out the inferior olive as a cause of OPT.

Harmaline and OPT

Studies of animal models of tremor have reported wide-spread, or even global, rhythmic oscillations (at 8-12 Hz) among inferior olive neurons induced by harmaline (De and Lamarre, 1973; Batini *et al.*, 1979; Bernard *et al.*, 1984; Miwa *et al.*, 2000). Yet, harmaline does not induce OPT (Kane and Thach, 1989). Unlike the synchronous oscillations of sets of coupled inferior olive cells in OPT that we have proposed, harmaline-induced tremors are generated by inferior olive over-excitation following the stimulation of the NMDA receptors on individual inferior olive neurons (Sinton *et al.*, 1989; Du *et al.*, 1997). The rhythmic firing after harmaline also begins within a few minutes, and thus cannot be due to hypertrophic changes in the inferior olive, which take weeks to months to develop. Thus, harmaline-induced tremor is not an appropriate model for OPT. Furthermore, as our model shows, a synchronous 10 Hz oscillation is not required for OPT, and thus the harmaline studies do not rule out a role for the inferior olive in OPT.

OPT and muscles derived from the branchial arch

OPT is most commonly (but not exclusively) associated with tremor in branchiomeric muscles, i.e. muscles derived ontologically from the branchial arch (Leigh and Zee, 2006). Kane and Thach (1989) pointed out that the olive and cerebellar cortex and deep nuclei are topographically mapped, and do not seem to favour the branchial cleft musculature. In their discussion Kane and Thach ascribed palatal myoclonus to a lesion in the central tegmental tract. The central tegmental tract projects to the inferior olive, but also to nearby areas of the brain, in particular the nucleus ambiguus. They argued that it is because the central tegmental tract lesion causes hypersensitivity of the nucleus ambiguus (known to innervate branchial muscles in the palate) that a 1-2 Hz oscillation develops. However, hypersensitivity by itself need not result in an oscillation of a particular frequency. In our model, it is the biophysical properties of the cell membranes, and the synchrony resulting from the gap junctions, which cause the synchronous ~2 Hz oscillations in the inferior olive. Even then, without the amplification from cerebellar learning, there would be no OPT. Thus, the nucleus ambiguus idea of Kane and Thach (1989) does not, as yet, provide a complete mechanism for palatal tremor, let alone OPT.

It should also be noted that others have pointed out that olivocerebellar circuit activity is geometrically complex and can change during a sequence of movements (Welsh *et al.*, 1995). Thus, it may not be possible to rule out an organization of the olivocerebellar circuitry associated with branchiomeric muscles. Nonetheless, now that we are proposing that the inferior olive is indeed involved in OPT, we must answer the question: why do inferior olive oscillations seem to affect mostly branchiomeric musculature?

One hypothesis is that the muscles involved tend not to have (or need) stretch reflexes, as they normally perform their actions against relatively unchanging mechanical loads (e.g. the extraocular muscles). These muscles usually insert on bone at only one end, are of small diameter and deal with small loads (Stal and Lindman, 2000). In contrast, the muscles that are usually not involved insert into bone at both ends, experience changing mechanical loads and have a stretch reflex. Other parts of the motor system, such as the cerebellum and spinal cord, may be sufficiently different for muscles with these two functions that even if the inferior olive neurons related to them are oscillating, those oscillations are not amplified by the cerebellum and thus not clinically observable. Cases of OPT may occasionally be seen with low frequency tremor in other muscles, e.g. neck, trunk or extremities (Leigh and Zee, 2006); perhaps these occur when inferior olive oscillations are large enough to be detected without amplification by the cerebellum.

Slower cerebellar learning in OPT patients

Cerebellar learning, which depends upon the inferior olive, proceeds more slowly in OPT patients than in normal subjects (Martin *et al.*, 1996; Deuschl *et al.*, 1996). For example, in a motor adaptation paradigm the movement has an exponentially decaying mean error curve. However, the time constant in OPT patients was greater than normal, suggesting that learning was slower in these patients (Deuschl *et al.*, 1996; Martin *et al.*, 1996). The dual-mechanism hypothesis for OPT provides a hypothetical explanation for this slow learning. Presumably, learning of this type depends upon the coincident arrival in the cerebellar cortex of a conditioning stimulus (via mossy fibres) and an unconditioned stimulus, or teaching signal, via climbing fibres from the inferior

olive (Hong and Optican, 2008). Normally, the inferior olive neurons are all puttering along at about 2 Hz, but with random phases, and when an unconditioned stimulus arrives it is easy to get some of the inferior olive neurons to fire and send the teaching signal to the cerebellar cortex. In contrast, when the inferior olive is abnormal in OPT, most of the inferior olive neurons are strongly coupled, and fire synchronously at 2 Hz. Thus, when an unconditioned stimulus arrives, it is difficult to get just a few of the learning-related neurons to fire at that time, because of the strong, ongoing synchronous oscillation. This would reduce the probability that the arrival of the conditioned and unconditioned signal in the cerebellar cortex would be coincident. Nonetheless, on average the teaching signal would be correct, so learning would proceed, but more slowly than normal.

Therapeutic implications—some speculations

The dual mechanism model showed that reducing the gain of different compartments in the model had different effects. Specifically, reducing the modulation of cerebellar circuitry should decrease the learning-dependent modulation of the Purkinje neuron activity and thus reduce the oscillation amplitude. Cerebellar modulation of the deep cerebellar or vestibular nuclei might be reduced, e.g. with drugs that can diminish Purkinje cell modulation, either by enhancing GABA mediated inhibition (e.g. clonazepam, alprazolam, primidone and topiramate) or by reducing glutamatergic excitation (e.g. memantine or topiramate).

In the model, the oscillations only stopped completely after reducing the coupling among inferior olive neurons below 20%. Drugs that reduce electrotonic coupling amongst hypertrophied inferior olive neurons by blocking connexons (e.g. quinine, carbenoxolone or mefloquine) (De Zeeuw *et al.*, 1995; Srinivas *et al.*, 2001; Connors and Long, 2004; Cruikshank *et al.*, 2004; Placantonakis *et al.*, 2006) should reduce the amplitude and frequency of the oscillations.

If treatment with a single drug has a limited effect, combining drug therapies to attack both the inferior olive gap junctions and the cerebellar modulation might prove more effective.

Conclusion

Our results emphasize the role of electrotonic coupling in inferior olivary nuclei as the cause of the ~2 Hz oscillations, and the role of the cerebellum in modulating those oscillations to smooth and amplify them. Our model can account for almost all the variations in OPT reported in the literature, restoring confidence in the idea that hypertrophy of the inferior olive nuclei cause them to become the pacemaker of OPT oscillations. The main shortcoming of this study is in the model's inability to reproduce the specific waveforms that are unique to each patient. This may be because other areas in the brain are also affected in OPT, and the model would have to be extended to include other eye movement related areas of the brain to account for waveforms of individual patients. The model predicts that pharmacological interventions with agents that reduce inferior olive synchronization, or reduce Purkinje cell disinhibition of the deep cerebellar nuclei, or both, would be therapeutic for OPT patients.

Acknowledgements

The authors thank Drs M. Hallett, C. Quaia and R. Llinás, and the anonymous referees for helpful discussions and suggestions.

Funding

Office of Research and Development, Medical Research Service, Department of Veterans Affairs; National Eye Institute (grants EY01849, EY06717 and EY08060); Evenor Armington Fund; Intramural Research Program, National Eye Institute, NIH, DHHS; Philanthropic funds to the JHH vestibular laboratory and JHH movement disorders division (Fellowship support to A.S.).

Supplementary material

Supplementary material is available at *Brain* online.

References

Andersson G, Oscarsson O. Projections to lateral vestibular nucleus from cerebellar climbing fiber zones. Exp Brain Res 1978; 32: 549–64.

Angaut P, Sotelo C. Synaptology of the cerebello-olivary pathway. Double labelling with anterograde axonal tracing and GABA immunocytochemistry in the rat 1. Brain Res 1989; 479: 361–5.

Averbuch-Heller L, Zivotofsky AZ, Remler BF, Das VE, Dell'Osso LF, Leigh RJ. Convergent–divergent pendular nystagmus: possible role of the vergence system. Neurology 1995; 45: 509–15.

Baker K, Warren KS, Yellen G, Fishman MC. Defective ''pacemaker'' current (Ih) in a zebrafish mutant with a slow heart rate. Proc Natl Acad Sci USA 1997; 94: 4554–9.

Balaban CD. Distribution of inferior olivary projections to the vestibular nuclei of albino rabbits. Neuroscience 1988; 24: 119–34.

Barmack NH. Central vestibular system: vestibular nuclei and posterior cerebellum 2. Brain Res Bull 2003; 60: 511–41.

Batini C, Buisseret-Delmas C, Conrath-Verrier M. Olivo-cerebellar activity during harmaline-induced tremor. A 2-[14C]deoxyglucose study. Neurosci Lett 1979; 12: 241–6.

Bengtsson F, Svensson P, Hesslow G. Feedback control of Purkinje cell activity by the cerebello-olivary pathway. Eur J Neurosci 2004; 20: 2999–3005.

Bernard JF, Buisseret-Delmas C, Compoint C, Laplante S. Harmaline induced tremor. III. A combined simple units, horseradish peroxidase, and 2-deoxyglucose study of the olivocerebellar system in the rat. Exp Brain Res 1984; 57: 128–37.

Birbamer G, Gerstenbrand F, Aichner F, Buchberger W, Chemelli A, Langmayr J, et al. MR-imaging of post-traumatic olivary hypertrophy. Funct Neurol 1994; 9: 183–7.

Carpenter MB, Stein BM, Peter P. Primary vestibulocerebellar fibers in the monkey: distribution of fibers arising from distinctive cell groups of the vestibular ganglia. Am J Anat 1972; 135: 221–49.

Connors BW, Long MA. Electrical synapses in the mammalian brain. Annu Rev Neurosci 2004; 27: 393–418.

Cruikshank SJ, Hopperstad M, Younger M, Connors BW, Spray DC, Srinivas M. Potent block of Cx36 and Cx50 gap junction channels by mefloquine 1. Proc Natl Acad Sci USA 2004; 101: 12364–9.

De Zeeuw CI, Chorev E, Devor A, Manor Y, Van Der Giessen RS, De Jeu MT, et al. Deformation of network connectivity in the inferior olive of connexin 36-deficient mice is compensated by morphological and electrophysiological changes at the single neuron level. J Neurosci 2003; 23: 4700–11.

De Zeeuw CI, Hertzberg EL, Mugnaini E. The dendritic lamellar body: a new neuronal organelle putatively associated with dendrodendritic gap junctions. J Neurosci 1995; 15: 1587–604.

De Zeeuw CI, Holstege JC, Ruigrok TJ, Voogd J. Ultrastructural study of the GABAergic, cerebellar, and mesodiencephalic innervation of the cat medial accessory olive: anterograde tracing combined with immunocytochemistry. J Comp Neurol 1989; 284: 12–35.

De Zeeuw CI, Ruigrok TJ, Schalekamp MP, Boesten AJ, Voogd J. Convergent–divergent pendular nystagmus: possible role of the vergence system. Eur J Morphol 1990; 28: 240–55.

De Zeeuw CI, Simpson JI, Hoogenraad CC, Galjart N, Koekkoek SK, Ruigrok TJ. Microcircuitry and function of the inferior olive. Trends Neurosci 1998; 21: 391–400.

De MC, Lamarre Y. Rhythmic activity induced by harmaline in the olivocerebello-bulbar system of the cat. Brain Res 1973; 53: 81–95.

Deuschl G, Mischke G, Schenck E, Schulte-Monting J, Lucking CH. Symptomatic and essential rhythmic palatal myoclonus. Brain 1990; 113(Pt 6): 1645–72.

Deuschl G, Toro C, Hallett M. Symptomatic and essential palatal tremor. 2. Differences of palatal movements 1. Mov Disord 1994a; 9: 676–8.

Deuschl G, Toro C, Valls-Sole J, Zeffiro T, Zee DS, Hallett M. Symptomatic and essential palatal tremor. 1. Clinical, physiological and MRI analysis 3. Brain 1994b; 117(Pt 4): 775–88.

Deuschl G, Toro C, Zeffiro T, Massaquoi S, Hallett M. Adaptation motor learning of arm movements in patients with cerebellar disease 2. J Neurol Neurosurg Psychiatry 1996; 60: 515–9.

Du W, Aloyo VJ, Harvey JA. Harmaline competitively inhibits [3H]MK-801 binding to the NMDA receptor in rabbit brain. Brain Res 1997; 770: 26–9.

Faulstich M, van Alphen AM, Luo C, du LS, De Zeeuw CI. Oculomotor plasticity during vestibular compensation does not depend on cerebellar LTD 1. J Neurophysiol 2006; 96: 1187–95.

Goyal M, Versnick E, Tuite P, Cyr JS, Kucharczyk W, Montanera W, et al. Hypertrophic olivary degeneration: metaanalysis of the temporal evolution of MR findings. AJNR Am J Neuroradiol 2000; 21: 1073–7.

Gresty MA, Ell JJ, Findley LJ. Acquired pendular nystagmus: its characteristics, localising value and pathophysiology. J Neurol Neurosurg Psychiatry 1982; 45: 431–9.

Hakimian S, Norris SA, Greger B, Keating JG, Anderson CH, Thach WT. Time and frequency characteristics of Purkinje cell complex spikes in the awake monkey performing a nonperiodic task. J Neurophysiol 2008; 100: 1032–40.

Hong S, Leigh RJ, Zee DS, Optican LM. Inferior olive hypertrophy and cerebellar learning are both needed to explain ocular oscillations in oculopalatal tremor. Prog Brain Res 2008a; 171: 219–26.

Hong S, Leigh RJ, Zee DS, Optican LM. Inferior olive hypertrophy and cerebellar learning are both needed to explain ocular oscillations in oculopalatal tremor 2. Prog Brain Res 2008b; 171: 219–26.

Hong S, Optican LM. Interaction between Purkinje cells and inhibitory interneurons may create adjustable output waveforms to generate timed cerebellar output. PLoS ONE 2008; 3: e2770.

Kane SA, Thach WT Jr. Palatal myoclonus and function of the inferior olive: are they related? In: Strata P, editor. Experimental brain research series. Berlin: Springer 1989; p. 427–60.

Keating JG, Thach WT. Nonclock behavior of inferior olive neurons: interspike interval of Purkinje cell complex spike discharge in the awake behaving monkey is random. J Neurophysiol 1995; 73: 1329–40.

Keating JG, Thach WT. No clock signal in the discharge of neurons in the deep cerebellar nuclei. J Neurophysiol 1997; 77: 2232–4.

Kim JS, Moon SY, Choi KD, Kim JH, Sharpe JA. Patterns of ocular oscillation in oculopalatal tremor: imaging correlations. Neurology 2007; 68: 1128–35.

Koeppen AH, Barron KD, Dentinger MP. Olivary hypertrophy: histochemical demonstration of hydrolytic enzymes. Neurology 1980; 30: 471–80.

Lapresle J. Palatal myoclonus. Adv Neurol 1986; 43: 265–73.

Leigh RJ, Zee DS. The neurology of eye movements. Oxford: Oxford University Press; 2006.

Liao K, Hong S, Zee DS, Optican LM, Leigh RJ. Impulsive head rotation resets oculopalatal tremor: examination of a model. Prog Brain Res 2008; 171: 227–34.

Llinas R, Baker R, Sotelo C. Electrotonic coupling between neurons in cat inferior olive 1. J Neurophysiol 1974; 37: 560–71.

Llinas R, Yarom Y. Oscillatory properties of guinea-pig inferior olivary neurones and their pharmacological modulation: an in vitro study 1. J Physiol 1986; 376: 163–82.

Llinas RR. Inferior olive oscillation as the temporal basis for motricity and oscillatory reset as the basis for motor error correction. Neuroscience 2009; 162: 797–804.

Manor Y, Rinzel J, Segev I, Yarom Y. Low-amplitude oscillations in the inferior olive: a model based on electrical coupling of neurons with heterogeneous channel densities. J Neurophysiol 1997; 77: 2736–52.

Martin TA, Keating JG, Goodkin HP, Bastian AJ, Thach WT. Throwing while looking through prisms. I. Focal olivocerebellar lesions impair adaptation. Brain 1996; 119(Pt 4): 1183–98.

Matsuo F, Ajax ET. Palatal myoclonus and denervation supersensitivity in the central nervous system. Ann Neurol 1979; 5: 72–8.

Miwa H, Nishi K, Fuwa T, Mizuno Y. Differential expression of c-fos following administration of two tremorgenic agents: harmaline and oxotremorine. Neuroreport 2000; 11: 2385–90.

Nakada T, Kwee IL. Oculopalatal myoclonus. Brain 1986; 109(Pt 3): 431–41.

Nishie M, Yoshida Y, Hirata Y, Matsunaga M. Generation of symptomatic palatal tremor is not correlated with inferior olivary hypertrophy. Brain 2002; 125: 1348–57.

Placantonakis DG, Bukovsky AA, Aicher SA, Kiem HP, Welsh JP. Continuous electrical oscillations emerge from a coupled network: a study of the inferior olive using lentiviral knockdown of connexin 36. J Neurosci 2006; 26: 5008–16.

Robinson DA. The use of matrices in analyzing the three-dimensional behavior of the vestibulo-ocular reflex. Biol Cybern 1982; 46: 53–66.

Ruigrok TJ, De Zeeuw CI, Voogd J. Hypertrophy of inferior olivary neurons: a degenerative, regenerative or plasticity phenomenon. Eur J Morphol 1990; 28: 224–39.

Ruigrok TJH. Cerebellar nuclei: the olivary connection. In: De Zeeuw CI, Strata P, Voogd J, editors. Progress in brain research. Amsterdam: Elsevier 1997; p. 167–92.

Schneiderman N, Fuentes I, Gormezano I. Acquisition and extinction of the classically conditioned eyelid response in the albino rabbit. Science 1962; 136: 650–2.

Schweighofer N, Doya K, Fukai H, Chiron JV, Furukawa T, Kawato M. Chaos may enhance information transmission in the inferior olive. Proc Natl Acad Sci USA 2004; 101: 4655–60.

Schweighofer N, Doya K, Kawato M. Electrophysiological properties of inferior olive neurons: A compartmental model. J Neurophysiol 1999; 82: 804–17.

Sinton CM, Krosser BI, Walton KD, Llinas RR. The effectiveness of different isomers of octanol as blockers of harmaline-induced tremor. Pflugers Arch 1989; 414: 31–6.

Sotelo C. Neuronal transplantation: Purkinje cell replacement and reconstruction of a defective cerebellar circuitry in mice with heredodegenerative ataxia. Boll Soc Ital Biol Sper 1986; 62: 1479–85.

Sotelo C, Llinas R, Baker R. Structural study of inferior olivary nucleus of the cat: morphological correlates of electrotonic coupling 2. J Neurophysiol 1974; 37: 541–59.

Sperling MR, Herrmann C Jr. Syndrome of palatal myoclonus and progressive ataxia: two cases with magnetic resonance imaging. Neurology 1985; 35: 1212–4.

Srinivas M, Hopperstad MG, Spray DC. Quinine blocks specific gap junction channel subtypes. Proc Natl Acad Sci USA 2001; 98: 10942–7.

Stal PS, Lindman R. Characterisation of human soft palate muscles with respect to fibre types, myosins and capillary supply 1. J Anat 2000; 197(Pt 2): 275–90.

Thach WT. Discharge of cerebellar neurons related to two maintained postures and two prompt movements. I. Nuclear cell output. J Neurophysiol 1970; 33: 527–36.

Welsh JP, Lang EJ, Suglhara I, Llinas R. Dynamic organization of motor control within the olivocerebellar system. Nature 1995; 374: 453–7.

Welsh JP, Yamaguchi H, Zeng XH, Kojo M, Nakada Y, Takagi A, et al. Normal motor learning during pharmacological prevention of Purkinje cell long-term depression. Proc Natl Acad Sci USA 2005; 102: 17166–71.

Westheimer G, McKee SP. Visual acuity in the presence of retinal-image motion. J Opt Soc Am 1975; 65: 847–50.

Yakushiji Y, Otsubo R, Hayashi T, Fukuchi K, Yamada N, Hasegawa Y, et al. Glucose utilization in the inferior cerebellar vermis and ocular myoclonus. Neurology 2006; 67: 131–3.

Yokota T, Tsukagoshi H. Olivary hypertrophy precedes the appearance of palatal myoclonus. J Neurol 1991; 238: 408.

Zhang Y, Partsalis AM, Highstein SM. Properties of superior vestibular nucleus neurons projecting to the cerebellar flocculus in the squirrel monkey. J Neurophysiol 1993; 69: 642–5.